NATIONAL ADVISORY COMMITTEE
FOR AERONAUTICS

TECHNICAL NOTE 4393

SOME STATIC LONGITUDINAL STABILITY CHARACTERISTICS

OF AN OVERLAPPED-TYPE TANDEM-ROTOR

HELICOPTER AT LOW AIRSPEEDS

By Robert J. Tapscott

Langley Aeronautical Laboratory
Langley Field, Va.

NACA

Washington

September 1958

1Z

NATIONAL ADVISORY COMMITTEE FOR AERONAUTICS

TECHNICAL NOTE 4393

SOME STATIC LONGITUDINAL STABILITY CHARACTERISTICS

OF AN OVERLAPPED-TYPE TANDEM-ROTOR

HELICOPTER AT LOW AIRSPEEDS

By Robert J. Tapscott

SUMMARY

Flight measurements of some longitudinal static stability characteristics with an overlapped-type tandem-rotor helicopter at low airspeeds are presented. The data show that a critical amount of longitudinal control is required to maintain trimmed flight at certain combinations of airspeed and rate of descent. Estimates based on theoretically predicted interference effects indicate that the front rotor downwash acting on the rear rotor could cause variation of the longitudinal moments of the same order of magnitude as the measured variation.

INTRODUCTION

Studies of the stability characteristics of both single- and tandem-rotor helicopters are being conducted to verify the continuing applicability of the existing criteria and, possibly, to reveal the need for additional criteria to cover specific items. Experience with two types of tandem-rotor helicopters (nonoverlapped no-vertical-gap type and overlapped with vertical-gap type) has shown that, in general, these helicopters are subject to the same criteria in order to have satisfactory flight handling qualities.

One characteristic noted with an overlapped-rotor tandem helicopter which was not included in previous studies of a nonoverlapped-rotor helicopter (refs. 1 and 2) is the apparent instability with airspeed as reflected by the unstable slope of the curve of longitudinal control position plotted against airspeed at certain low airspeed conditions (0- to 25-knot range). In addition, with the airspeed constant in the low range, a large longitudinal trim change appears to result when the rate of descent (power) is varied within certain limits.

Information should be provided for the designer to indicate the possible occurrence of these characteristics and the mechanism by which

they occur so that consideration can be given during the design stages
to minimize them or shift them to a little-used flight condition. Some
recent studies of longitudinal stability characteristics at the low end
of the airspeed range are reported herein for an overlapped-type tandem-
rotor helicopter.

SYMBOLS

V_v vertical component of helicopter velocity along flight path,
           positive for climb, fps

V_h horizontal component of helicopter velocity along flight path,
           knots or fps as indicated

R   blade radius, ft

Ω rotor angular velocity, radians/sec

v   average induced inflow velocity of isolated rotor, always
           positive, fps

Δv difference between induced velocities of front and rear
           rotors, positive when rear rotor value is greater, fps

λ inflow ratio, assumed herein equal to $\dfrac{-V_v - v}{\Omega R}$

$\Delta\lambda$ difference between inflow ratios of front and rear rotors,
           positive when inflow ratio of rear rotor is greater

T   rotor thrust, component of rotor resultant force parallel to
           axis of no feathering, lb

ρ mass density of air, slugs/cu ft

μ tip-speed ratio, assumed to be equal to $V_h/\Omega R$

X   angle between axis of wake and normal to tip-path plane,

           approximately $\tan^{-1} \dfrac{-\mu}{\lambda}$

θ blade-section pitch angle; angle between line of zero lift of
           blade section and plane perpendicular to axis of no feath-
           ering, deg

$\Delta\theta$ difference between collective pitch angles of front and rear
rotors, positive when pitch of rear rotor is greater, deg

C_T rotor-thrust coefficient, $\dfrac{T}{\pi R^2 \rho (\Omega R)^2}$

v_{hov} average induced velocity of isolated rotor in hovering flight,
always positive, fps

A bar over a symbol indicates a parameter expressed as a ratio to
hovering induced velocity v_{hov}. For example, $\bar{v} = \dfrac{v}{v_{hov}}$.

DESCRIPTION OF HELICOPTER AND EQUIPMENT

A three-view drawing showing the general arrangement and principal
dimensions of the helicopter used for these studies is shown in figure 1.
The approximate physical characteristics are listed in table I. The
helicopter has conventional controls: cyclic pitch stick, directional
control pedals, and collective pitch stick with throttle control. Longi-
tudinal control is accomplished by longitudinal cyclic pitch and differ-
ential collective pitch, the latter providing about 85 percent of the
pitching moment. A calibration of the longitudinal cyclic pitch and the
differential collective pitch for a neutral setting of the trim control
is shown in figure 2. This calibration provides a means of converting
the control-stick positions to actual values of pitch on the rotors.

The helicopter was equipped with synchronized standard NACA recording
instruments that recorded control position, altitude, airspeed, linear
and angular accelerations about the three principal axes of inertia, and
angle of attack at the nose of the helicopter of the plane perpendicular
to the rotor shafts.

For most of the data discussed in this paper, the center of gravity
of the helicopter was located 4 inches forward of the midpoint between
rotors (station 178). A small part of the data, as noted on the pertinent
figures, were obtained with the center of gravity located 13 inches for-
ward of the midpoint between rotors (station 169). For measurements of
an airspeed component at near zero or negative values, a somewhat unique
pickup system was installed on the helicopter. The airspeed installation
is described in the appendix. Altitude and vertical velocity were
obtained from a static-pressure source independent of the airspeed system.
This source consisted of a static-pressure pickup on a swivel mounting at
the end of a boom extending forward of the fuselage nose.

FLIGHT MEASUREMENTS OF LONGITUDINAL STABILITY

CHARACTERISTICS AT LOW AIRSPEEDS

Stability With Speed

The stability with speed of the helicopter at low airspeeds was
studied by means of the following procedure: The helicopter was trimmed
in forward flight at an airspeed of about 25 knots at a given power. A
range of airspeed (approximately -10 to 40 knots) was traversed by slowly
and continuously reducing airspeed to the minimum at a rate of about
1 knot per second, then increasing to about 40 knots, and reducing again
to the starting trim value. The collective pitch and throttle settings
were kept constant throughout each cycle of airspeed variation. Data
obtained from records of longitudinal control position during the cycle
of airspeed variation, when plotted against airspeed, are then indica-
tive of the change in longitudinal pitching moments acting on the heli-
copter with change in airspeed from a trimmed value; that is, they are
indicative of the stability with airspeed of the helicopter.

The variation of stick position with airspeed for the subject heli-
copter at several power conditions is shown in figure 3. The power con-
ditions are designated A, B, C, and D, and are defined in table II in
terms of the resulting trimmed flight parameters. As illustrated by the
plots of figure 3 the helicopter is generally slightly unstable with air-
speed above about 20 knots and becomes relatively stable below about
20 knots for all power conditions shown except power condition B. For
power condition B, with decreasing airspeed, the helicopter apparently
undergoes a relatively large nose-up trim change at about 15 knots which
requires nearly full nose-down control to overcome.

In figure 4 plots are presented showing the variation with airspeed
of the rate of change of altitude (V_v) for the cases shown in figure 3.
These plots show, in general, that different rates of descent may result
at the same airspeed and power, depending upon whether the airspeed is
slowly increasing or decreasing. Thus, in this case, the technique of
slowly varying airspeed at constant power and collective pitch does not
provide a reliable or repeatable means of obtaining speed stability data.

Trim Change With Vertical Velocity

In an effort to define further the flight conditions for which the
extreme forward (or nose-down) longitudinal control is required for trim,
control position records were obtained for steady rates of climb and
descent at two airspeeds. These data are shown in figure 5 as plots of
control position against vertical velocity for indicated airspeeds of

13 knots and 25 knots. It is shown by these plots that at each airspeed the control position required for trim is influenced by the vertical velocity; thus, at constant airspeed a trim change with power is indicated.

Figure 5 shows that, at each airspeed considered, increasingly forward control positions are required for trim as the vertical velocity decreases until values of about -10 feet per second (that is, descending) are reached. For vertical velocities greater than -10 feet per second (higher rates of descent), the trend of control positions for trim is rearward. The plots in figures 5(a) and 5(b) for 13 knots and for 25 knots, respectively, show generally similar trends. There does, however, appear to be a tendency for the maximum forward control position for trim to occur at slightly more negative vertical velocities and to be farther forward for the 13-knot airspeed than for the 25-knot airspeed.

Significance of Measured Characteristics

Existing criteria for satisfactory flying qualities for helicopters (for example, refs. 3 and 4) indicate the desirability of positive static longitudinal control position stability with speed at all steady flight conditions. The presence at low airspeeds of instability with speed and of large longitudinal trim changes with power conflicts with the especial need for good handling characteristics during the landing approach maneuver. Thus, of possible importance to the immediate safety of a given design configuration are the large trim changes with power in the low airspeed range presented in the previous section. The flight measurements indicate the possibility that critical amounts of longitudinal control may be required at certain combinations of airspeed and power. Should the critical combinations be within the range used during power-on landing approaches, dangerous flight attitudes can result with insufficient longitudinal control remaining for recovery. The possible need for excessive control at any flight condition might also bear directly on autopilot performance and particularly when the use of the autopilot is considered in conjunction with an approach coupler or other automatic landing approach devices.

It may be desirable, in order to provide added awareness on the part of the designer of a new configuration of the possibility of insufficient longitudinal control at some flight condition, to emphasize in future criteria the need for investigation of sufficient combinations of power and airspeed to insure that critical amounts of longitudinal control have been determined. It may not be feasible to eliminate completely all trim changes or excessive control requirements. However, it may be possible by proper selection of design variables to provide a safe margin of control at the critical combinations of power and airspeed and to set these critical combinations at a little-used flight condition.

COMPARISON OF FLIGHT MEASUREMENTS AND THEORETICAL

ESTIMATES OF TRIM CHANGE

It is believed that the measured characteristics which have been presented reflect both the effects of direct mutual interference between the flow fields of the two rotors and the effects of one or both rotors approaching the vortex-ring flow state. It is considered desirable to show the correlation that exists between measured data and predicted effects of flow interference between the front and rear rotors and to point out that portion of the flight regime which should be affected by unsteady vortex-ring flow conditions.

Procedure for Predicting Trim Change

The net difference of interference-induced velocities at the front rotor and at the rear rotor was estimated from the charts of both references 5 and 6. The charts of reference 5 are based on the assumption of uniform local disk loading and those of reference 6 are based on an assumed triangular local disk loading. Thus, the effects of the two assumed disk loadings on calculated control position variations can be seen. Figure 6 shows plots of the ratio of the net average interference velocity to the average front-rotor induced velocity (positive for net effect on the rear rotor) against rotor wake angles. The velocity ratios were derived from the charts of both references 5 and 6 for the particular geometry (rotor spacing, vertical gap and overlap) of the helicopter used for these flight measurements. At each wake angle for which the charts are presented in references 5 and 6, the average value of the interference-induced velocity was determined by averaging the interference-induced velocities along the longitudinal center line of the rotors. It should be noted, in regard to the estimation of wake velocities in such a manner, that the use of the data for an assumed uniform loading (ref. 5) might be expected to provide a more representative value for interference purposes than would the use of data for an assumed triangular loading (ref. 6). This arises from the fact that, since only the induced velocities in a plane through the rotor center line are used, the assumed uniform loading results in a value of induced velocity at the rotor center which is more representative of an average along the lateral axis than the value of zero resulting from the assumed triangular loading.

The interference-induced velocities shown in figure 6 were considered to represent differences between the operating conditions of the front and rear rotors which required specific collective pitch differences to provide for no thrust differential between rotors, that is, no longitudinal moment acting on the helicopter. Calculation of the control position or differential collective pitch for a given flight condition, the center of gravity being midway between rotors and only rotor contributions being considered, was then accomplished with the following procedure:

The inflow differences between the front and rear rotors which reflect the interference-induced velocities were determined in the following manner: As defined herein,

$$\lambda = \frac{-V_v - v}{\Omega R}$$

$$\mu = \frac{V_h}{\Omega R}$$

where V_h is measured in feet per second. Expressing these parameters in terms of nondimensional velocities by dividing the appropriate terms by the hovering induced velocity $v_{hov} = \Omega R \sqrt{C_T/2}$ yields

$$\lambda = \left(-\overline{V}_v - \overline{v}\right)\sqrt{C_T/2}$$

$$\mu = \overline{V}_h \sqrt{C_T/2}$$

wherein a bar over a symbol represents the ratio of the parameter to the hovering induced velocity.

From reference 5, $X = \tan^{-1}\dfrac{-\mu}{\lambda}$ (neglecting flapping) which upon substituting the relationships for λ and μ becomes

$$X = \tan^{-1} \frac{\overline{V}_h}{\overline{V}_v + \overline{v}}$$

Since the front and rear rotors are subject to the same vertical velocities $\overline{V}_v$, the difference in inflow ratio between the two rotors is caused by a difference in the induced-velocity parameter $\overline{v}$. Thus,

$$\Delta\lambda = -\Delta\overline{v}\sqrt{C_T/2}$$

or

$$\frac{\Delta\lambda}{\sqrt{C_T/2}} = -\overline{v}\,\frac{\Delta\overline{v}}{\overline{v}}$$

From the expression for the induced velocities,

$$v_{hov} = \Omega R \sqrt{C_T/2}$$

and

$$v = \Omega R \frac{C_T/2}{\sqrt{\lambda^2 + \mu^2}}$$

along with the definitions for λ and μ, the relationship between $\overline{V}_v$, $\overline{V}_h$, and $\overline{\overline{v}}$ becomes

$$\overline{\overline{v}} = \frac{1}{\sqrt{(\overline{V}_v + \overline{\overline{v}})^2 + \overline{V}_h{}^2}}$$

If these equations are summarized,

$$\frac{\Delta\lambda}{\sqrt{C_T/2}} = -\overline{\overline{v}}\, \frac{\Delta\overline{\overline{v}}}{\overline{\overline{v}}} \tag{1}$$

$$\chi = \tan^{-1} \frac{\overline{V}_h}{\overline{V}_v + \overline{\overline{v}}} \tag{2}$$

and

$$\overline{\overline{v}} = \frac{1}{\sqrt{(\overline{V}_v + \overline{\overline{v}})^2 + \overline{V}_h{}^2}} \tag{3}$$

From equations (1) to (3) it is seen, since $\Delta\overline{\overline{v}}/\overline{\overline{v}}$ is a function of the wake angle (fig. 6) and $\overline{\overline{v}}$ in equations (1) and (2) can be related to $\overline{V}_v$ and $\overline{V}_h$ by equation (3), that the parameter $\dfrac{\Delta\lambda}{\sqrt{C_T/2}}$ can be evaluated as a function of $\overline{V}_h$ and $\overline{V}_v$ alone. Thus, the difference in operating conditions of the front and rear rotors can be found for various combinations of forward velocity and vertical velocity $\left(\overline{V}_h \text{ and } \overline{V}_v, \text{ respectively}\right)$.

The parameter representing a change in differential collective pitch needed to keep the thrust difference between the front and rear rotors zero (that is, no longitudinal pitching moments) with an inflow difference on the rotors was calculated by the following relationship:

$$\frac{\Delta\theta}{\sqrt{C_T/2}} = -\frac{\partial\theta}{\partial C_T} \frac{\partial C_T}{\partial \lambda} \cdot \frac{\Delta\lambda}{\sqrt{C_T/2}}$$

The quantities $\partial\theta/\partial C_T$ and $\partial C_T/\partial\lambda$ are essentially constant throughout the low airspeed range ($\mu \leqq 0.1$) and, from the charts presented in reference 7, are estimated to be

$$\frac{\partial C_T}{\partial \lambda} = -0.0796$$

$$\frac{\partial \theta}{\partial C_T} = 1,130 \text{ deg/unit } C_T$$

In order to convert the parameter $\dfrac{\Delta\theta}{\sqrt{C_T/2}}$ to the actual cyclic pitch difference on the rotors, the average thrust coefficient should be used. In order to determine the actual control-stick travel for a given helicopter, a calibration of differential cyclic pitch with stick position, such as that shown in figure 2, can be used.

In the foregoing procedure fuselage and tail moments have been neglected and the longitudinal tilt of the rotor tip-path planes (longitudinal cyclic pitch) caused by control stick motion was neglected both in determining the relative positions of the rotors for estimating interference values from figure 6 and in determining the control positions needed to produce the necessary moments. Estimates of the probable contribution to the longitudinal moments of the fuselage and tail surfaces show that, for the flight conditions studied, the change in moments to be expected from this source is relatively small (about 5 percent of control authority) compared with the rotor moments. It is believed that the effects of tip-path-plane tilt would tend to be compensating and small, and thus the calculated control variation should be a reasonable estimate of the variations caused by rotor interference.

Comparison of Calculated and Measured Data

By using the procedure discussed in the previous section, control position variations with vertical velocity were calculated for the two forward airspeeds (13 knots and 25 knots) for which experimental data were presented in figure 5. The calculations were made by using the theoretical interference velocities for the two assumptions of uniform local disk loading and triangular disk loading. These data along with the measured control positions shown in figure 5 are shown in figure 7 as plots of the control parameter $\dfrac{\Delta\theta}{\sqrt{C_T/2}}$ against vertical velocity for the two speeds (designated nondimensionally as $\overline{V}_h = 0.85$ and 1.60) for which the measured data were obtained. The approximate region for which the front rotor is estimated to be affected by vortex-ring flow conditions is indicated in figure 7. The amount of nose-down control available on the test helicopter is also indicated on the figure. For the calculated curves only the control needed to overcome interference

effects between rotors is considered; thus, except for the data well into
the vortex-ring flow region, it appears from figure 7 that the major
trends of the measured variation of longitudinal trim changes can be
fairly well accounted for by predicted effects of front rotor wake acting
on the rear rotor.

At the smaller rates of descent, the measured data for $\overline{V}_h = 0.85$
(fig. 7(a)) and $\overline{V}_h = 1.60$ (fig. 7(b)) show a trend of nose-down or
forward-control position as the vertical velocity parameter is decreased
(descending) similar to that indicated by the calculations based on inter-
ference. As can be explained by the considerations previously noted, the
slope of the data more nearly agrees with the calculations based on uni-
form local disk loading. Once the front rotor is well into the region
for vortex-ring flow, there appears to be little correlation between the
measured trends and those predicted by either method. Although in this
region considerable scatter in the measured points is apparent, in gen-
eral the data show a trend toward rearward control. Such a trend might
be expected when the front rotor is operating sufficiently far into the
region identified with vortex-ring flow state to have an unstable varia-
tion of thrust with collective pitch.

It is possible that the proximity to the vortex-ring flow state
might also affect the degree of agreement of the measured and predicted
trends at the lower rates of descent. The agreement shown, however, is
considered sufficient to warrant the use of the method without such addi-
tional refinements for exploring the possibility of excessive longitudinal
control requirements at various flight conditions. The degree of agree-
ment also appears to be sufficient to warrant use of the method during
the design stages to examine potential control requirements at the most
severe condition of rotor interference and to aid in placing the condi-
tion for maximum control need at some little-used flight condition.

Theoretical Indications of the Effects of Rotor

Interference on Longitudinal Control

In order to explore the possibility of excessive longitudinal con-
trol requirements for a range of flight conditions, calculations were
made at one lower $\left(\overline{V}_h \approx 0.40\right)$ and one higher $\left(\overline{V}_h \approx 2.50\right)$ airspeed con-
dition than those for which experimental data were obtained. These data
are shown in figure 8 along with the two curves previously presented for
comparison purposes. As might be expected from the relative magnitudes
of the maximum interference-induced velocities shown in figure 6 for the
two assumed disk loadings, the estimates of control requirements shown
in figure 7 based on uniform local disk loading indicate the possibility
of much more severe maximum nose-down control requirement than those

estimates based on triangular local disk loading. Comparison of figures 8(a) and 8(b) shows that the trends of control required as airspeed and vertical velocity vary are similar for the two assumed variations of disk loading. The trends show that, at all airspeeds considered, large amounts of longitudinal control are predicted for trim at some rate of descent. The predicted curves also show the tendency, noted previously in the discussion of the experimental data, for the longitudinal control requirement to be more severe at the critical conditions for the lower airspeeds.

The curves for the lowest airspeed $\left(\overline{V}_h = 0.40\right)$ shown in figures 8(a) and 8(b) also suggest that more than one trim control position may exist at high rates of descent at that airspeed. The theory is known to be inadequate for calculating induced velocities in this region. An examination of values of induced velocity obtained from the semiempirical treatment of reference 8 for this airspeed region, however, appears to support the existence of more than one trim position.

CONCLUSIONS

The indications of some studies of static longitudinal stability and control characteristics of an overlapped tandem-rotor helicopter at low forward airspeeds can be summarized as follows:

1. Different rates of descent may be obtained at the same slowly changing forward airspeed and constant power depending upon whether the condition is approached from lower or higher airspeeds; thus, for very low airspeeds, the technique of slowly varying airspeed at constant power and collective pitch does not provide a reliable or repeatable means of obtaining reliable speed stability data.

2. At certain combinations of low forward airspeeds and power (rate of descent), a critical amount and rate of change with power of longitudinal control is required to maintain trimmed flight for the test configuration.

3. Estimates based on theoretically predicted interference between rotors operating in tandem show that the interference between the rotors at certain flight conditions could provide a potential source of larger moments than can be counteracted by amounts of longitudinal control generally provided for tandem configurations.

4. For a tandem configuration it appears desirable during the design stages to use theoretical procedures such as those provided herein to

examine the potential control requirement at the most severe condition
of rotor interference and to place the condition for maximum control
need at some little-used flight condition.

Langley Aeronautical Laboratory,
    National Advisory Committee for Aeronautics,
        Langley Field, Va., August 26, 1958.

APPENDIX

INSTALLATION FOR MEASURING LOW AIRSPEEDS

In order to provide a measurement of airspeed at near zero or nega-tive values, a system of four double-ended shielded tubes were installed on the helicopter. The locations at which the tubes were installed are noted in figure 1. A schematic diagram of the installation and details of the pickup tubes are shown in figure 9.

The pickup tubes were designed through wind-tunnel tests with the intent of providing a total-pressure and low-pressure reference source which would measure essentially a component of airspeed along the axis of the tube. For forward airspeeds the forward end of the tubes acted as pressure pickups, the rearward end supplying the low-pressure ref-erence. Conversely, for rearward airspeeds the rearward end of the tubes became pressure pickups, the forward end acting as a reference. Four locations were used to average out the effects of local flow varia-tions and to provide a basically symmetrical pickup system applicable to both forward and rearward airspeeds.

The pickup tubes were manifolded together and connected to the pilot's indicator and recorder. A calibration of the system was made in level flight by pacing the helicopter with a ground vehicle and by hovering in known wind velocities. This calibration, used to relate the flight condition to nondimensional air-flow parameters, is shown in figure 10. Figure 10 shows that the calibration of the system is approxi-mately linear above about 20 knots and indicates progressively higher than calibrated airspeed as the airspeed is increased. Also, the cali-bration of the airspeed system appears to be nonlinear below about 20 knots and provides an indicated airspeed of about 10 knots rearward for cali-brated zero airspeed. No calibration of the airspeed system was made in other than level flight; however, as already mentioned, the pickup tubes were developed to provide essentially a cosine-wave calibration of pres-sure difference against flow angle. Thus, the system should indicate a pressure difference approximately proportional only to the component of airspeed along the axis of the tubes. Pilot's comments during the flight tests showed that, in accordance with the initial design intention of the pickup tubes, the indications were relatively unaffected by vertical velocity.

REFERENCES

1. Amer, Kenneth B.: Some Flying-Qualities Studies of a Tandem Helicopter. NACA RM L51H20a, 1951.

2. Tapscott, Robert J., and Amer, Kenneth B.: Studies of the Speed Stability of a Tandem Helicopter in Forward Flight. NACA Rep. 1260, 1956. (Supersedes NACA RM L53F15a.)

3. Anon.: Helicopter Flying Qualities, Requirements for Military Specification MIL-H-8501, Nov. 5, 1952.

4. Anon.: Rotorcraft Airworthiness; Transport Categories. Pt. 7 of Civil Air Regulations, Civil Aero. Board, U. S. Dept. Commerce, Aug. 1, 1956.

5. Castles, Walter, Jr., and De Leeuw, Jacob Henri: The Normal Component of the Induced Velocity in the Vicinity of a Lifting Rotor and Some Examples of Its Application. NACA Rep. 1184, 1954. (Supersedes NACA TN 2912.)

6. Heyson, Harry H., and Katzoff, S.: Induced Velocities Near a Lifting Rotor With a Nonuniform Disk Loading. NACA Rep. 1319, 1957. (Supersedes NACA TN 3690 by Heyson and Katzoff and TN 3691 by Heyson.)

7. Gessow, Alfred, and Tapscott, Robert J.: Charts for Estimating Performance of High-Performance Helicopters. NACA Rep. 1266, 1956. (Supersedes NACA TN 3323 by Gessow and Tapscott and TN 3482 by Tapscott and Gessow.)

8. Amer, Kenneth B., and Gessow, Alfred: Charts for Estimating Tail-Rotor Contribution to Helicopter Directional Stability and Control in Low-Speed Flight. NACA Rep. 1216, 1955. (Supersedes NACA TN 3156.)
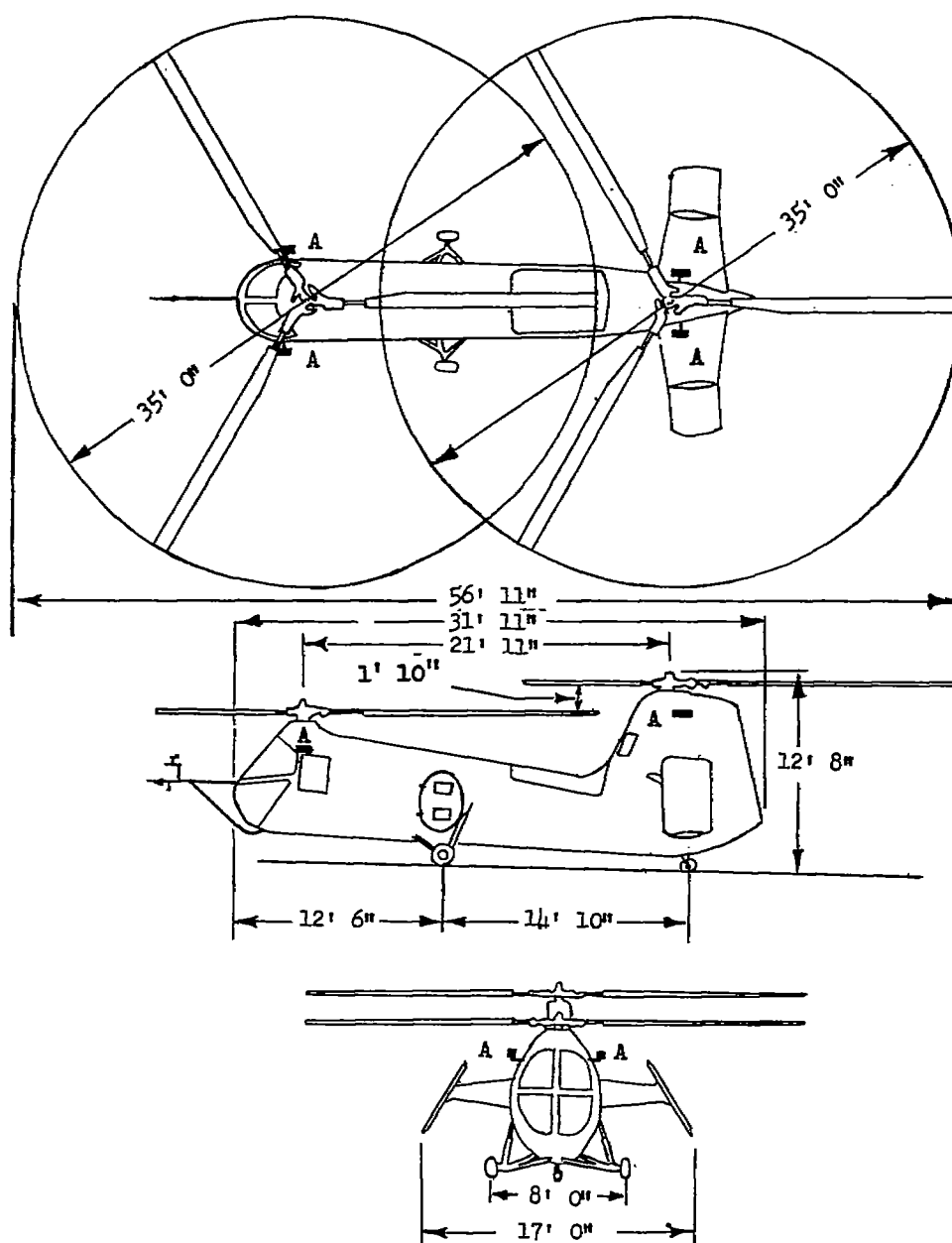
TABLE I

APPROXIMATE PHYSICAL CHARACTERISTICS OF HELICOPTER

Gross weight, lb 5,600
Thrust coefficient, C_T, average of both rotors 0.0055
Pitching moment of inertia, slug-ft^2 11,000
Number of blades per rotor 3
Diameter of each rotor, ft 35
Distance between rotor shafts, ft 21.9
Vertical distance between plane of rotors, ft 1.8
Solidity (chord weighted according to radius squared) 0.059
Blade mass constant (ratio of air forces to inertia
    forces) 7.5
Longitudinal cyclic pitch per inch of stick deflec-
    tion, deg 1.09
Differential collective pitch per inch of stick
    deflection, deg 0.68
Horizontal-stabilizer projected area, approximate, sq ft . . . 48
Total vertical-stabilizer projected area, approximate,
    sq ft 31
Allowable center-of-gravity range, inches forward of
    midpoint between rotors . . . . -7 to 13

TABLE II

DEFINITION OF POWER CONDITIONS IN TERMS OF

TRIMMED FLIGHT PARAMETERS

Designation of power condition	Trimmed values						
	Airspeed, V_h, knots	Vertical velocity, V_v, fps	Rotational velocity of -		Engine manifold pressure, in. Hg	Outside air temperature, °F	Pressure altitude, ft
			Rotor, rpm	Engine, rpm			
A	24	9	275	2,375	39	43	3,350
B	20	0	275	2,375	35	38	3,770
C	22	-8	275	2,375	30	45	3,200
D	25	-11	275	2,375	25	42	3,400

A   Airspeed pickup units
         (4 locations)

Figure 1.- Three-view drawing of helicopter used for flight measurements.
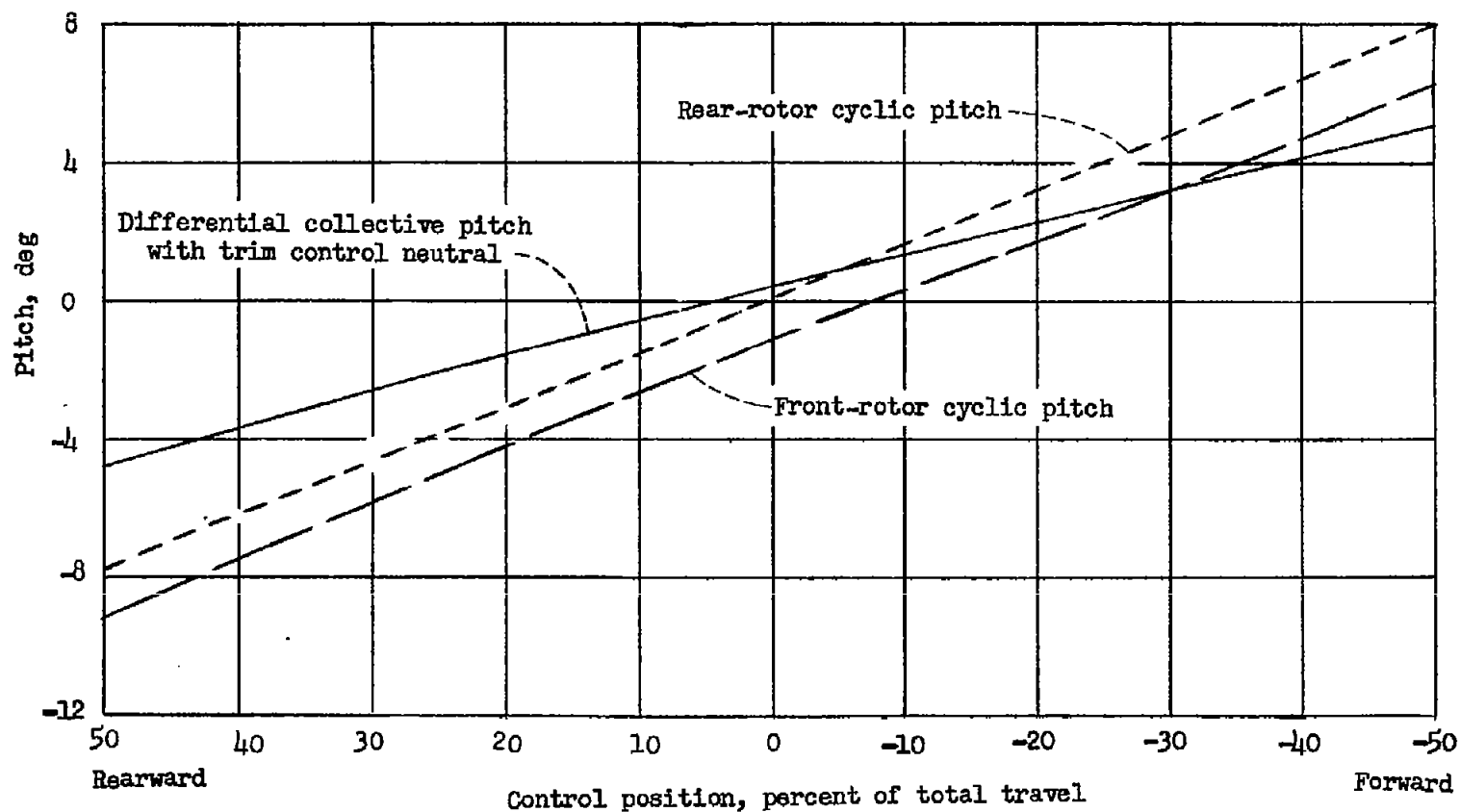
Figure 2.- Longitudinal control calibration for helicopter used for flight measurements.
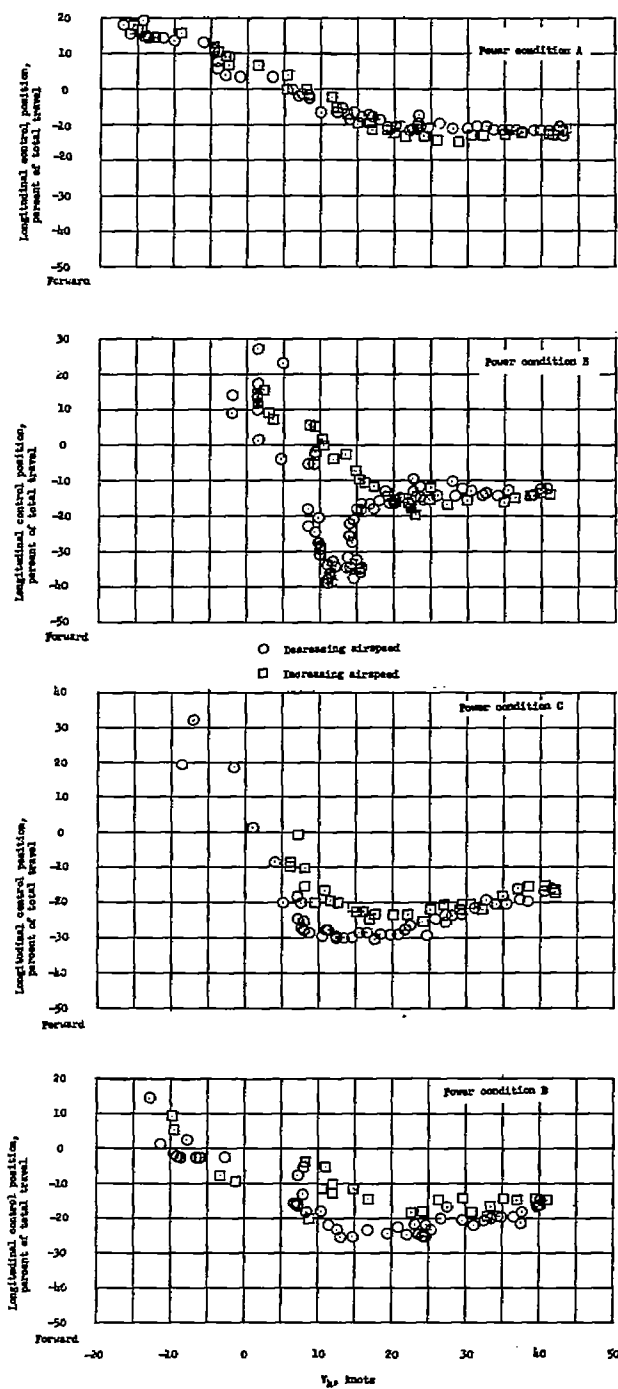
Figure 3.- Variation of longitudinal control position with airspeed for several power conditions. Power conditions are defined in table II.
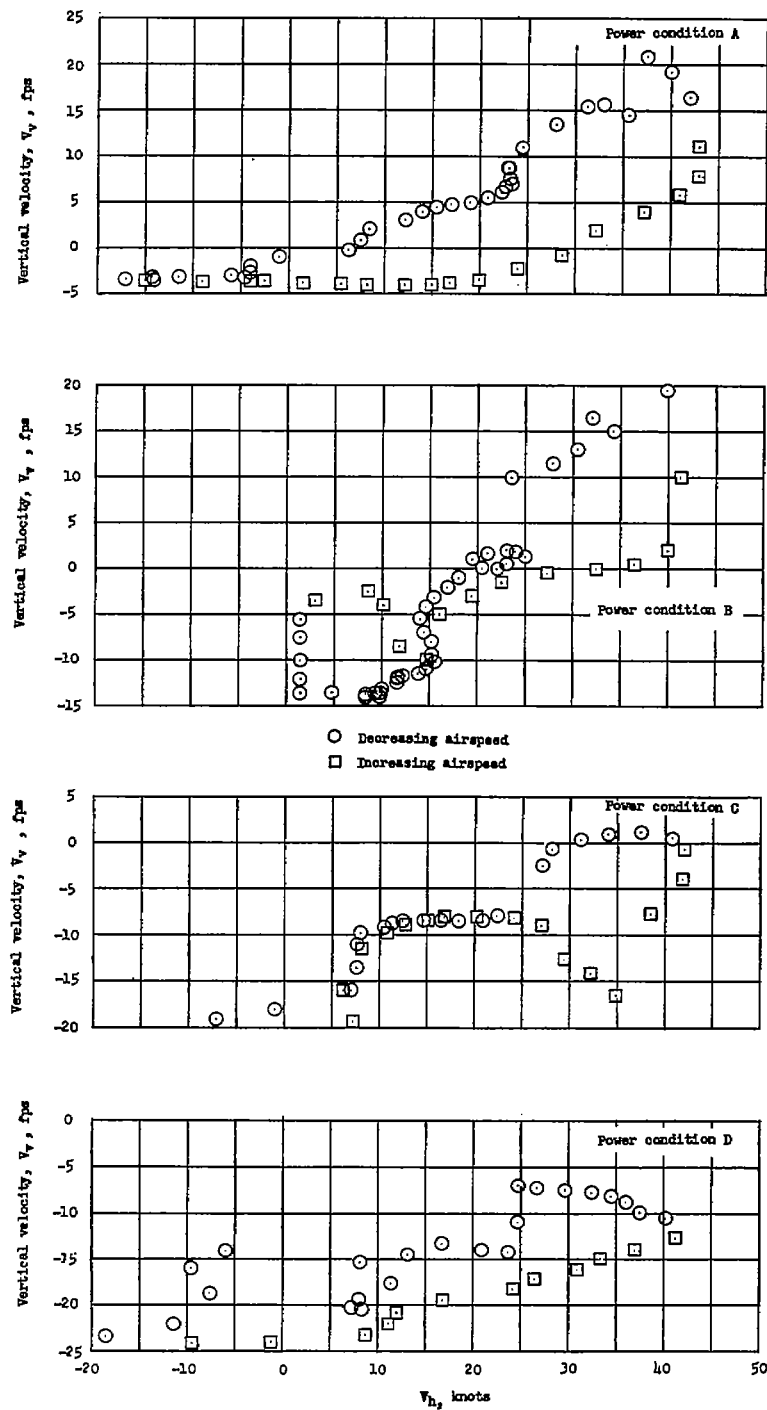
Figure 4.- Variation of vertical velocity with indicated airspeed for
several power conditions. Power conditions are defined in table II.
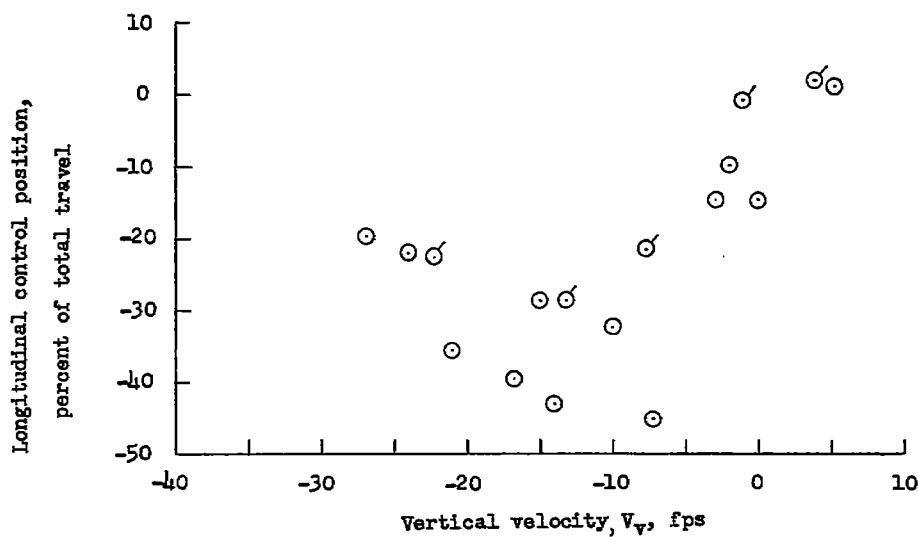
(a) 13 knots.

O Center of gravity, station 178

♂ Center of gravity, station 169
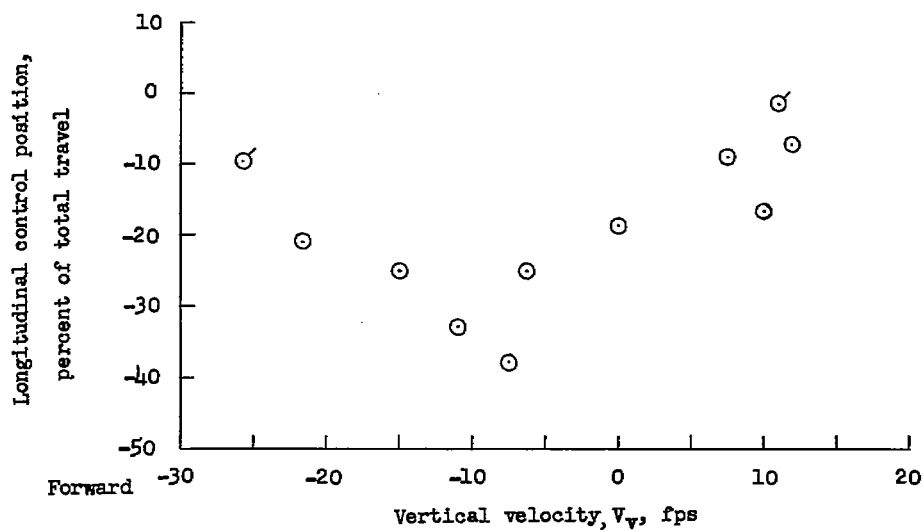
(b) 25 knots.

Figure 5.- Plots of longitudinal control position against vertical
velocity at constant indicated airspeed.
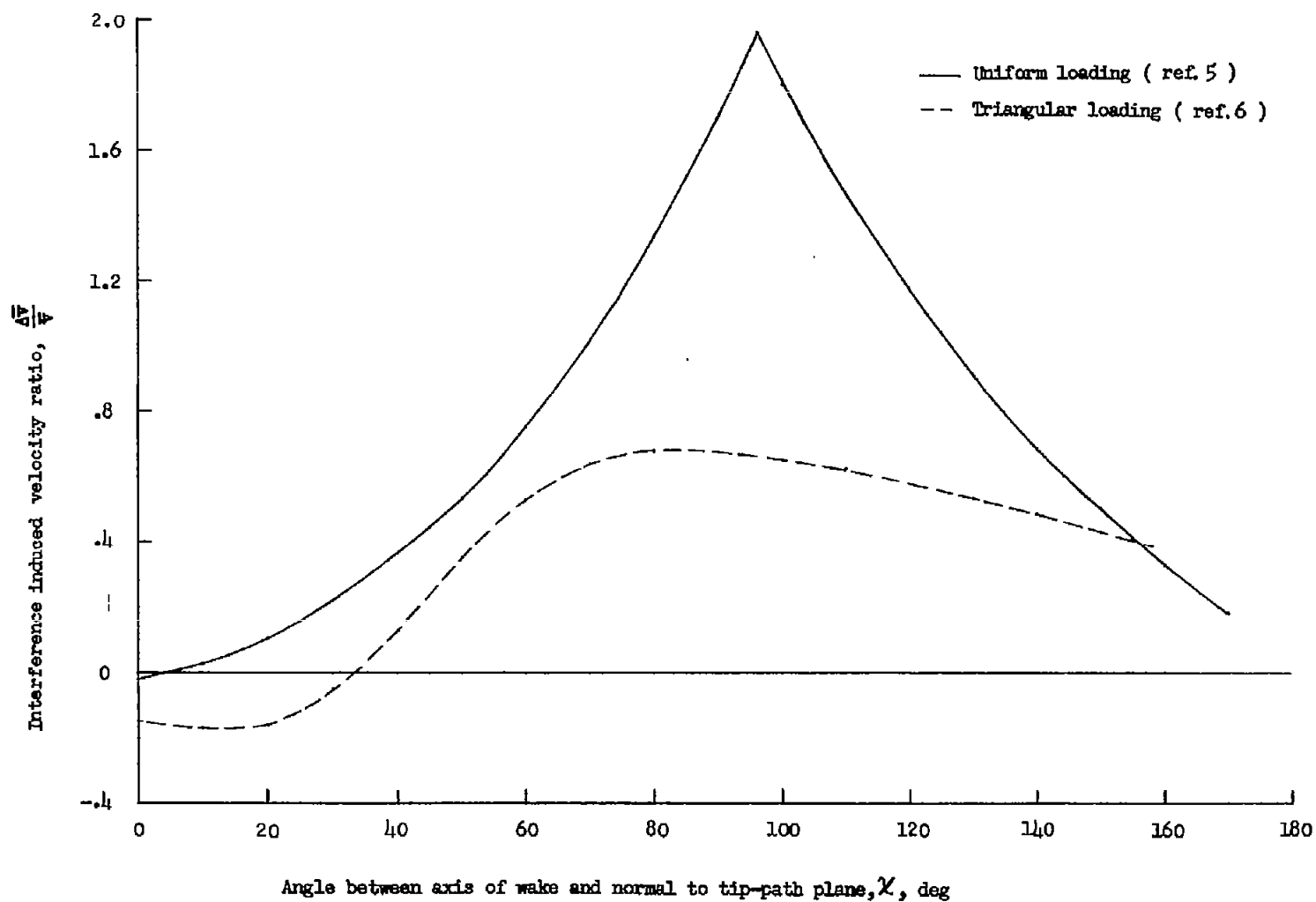
Figure 6.- Theoretical interference-induced velocity ratio for helicopter plotted against angle of front-rotor wake.
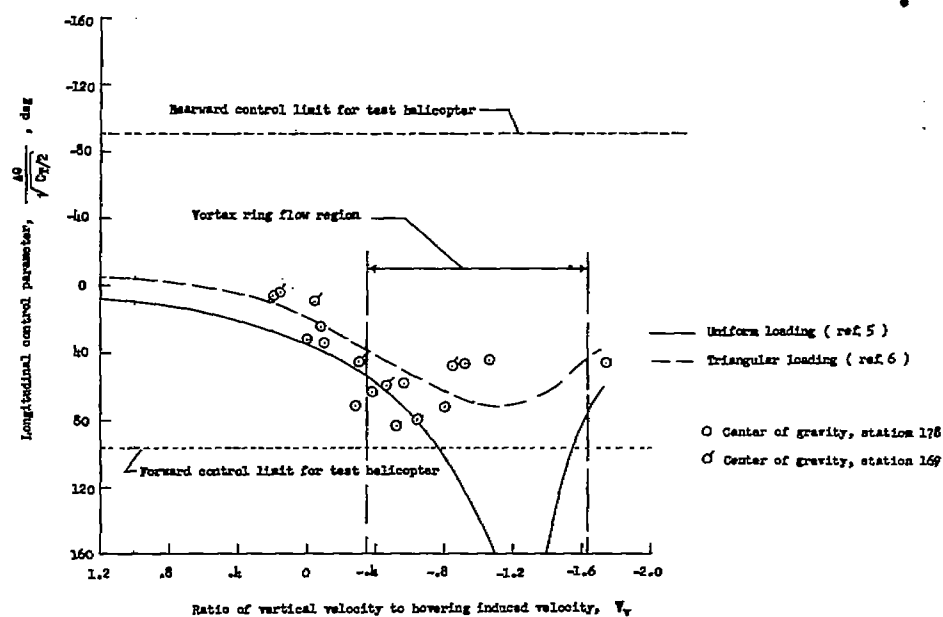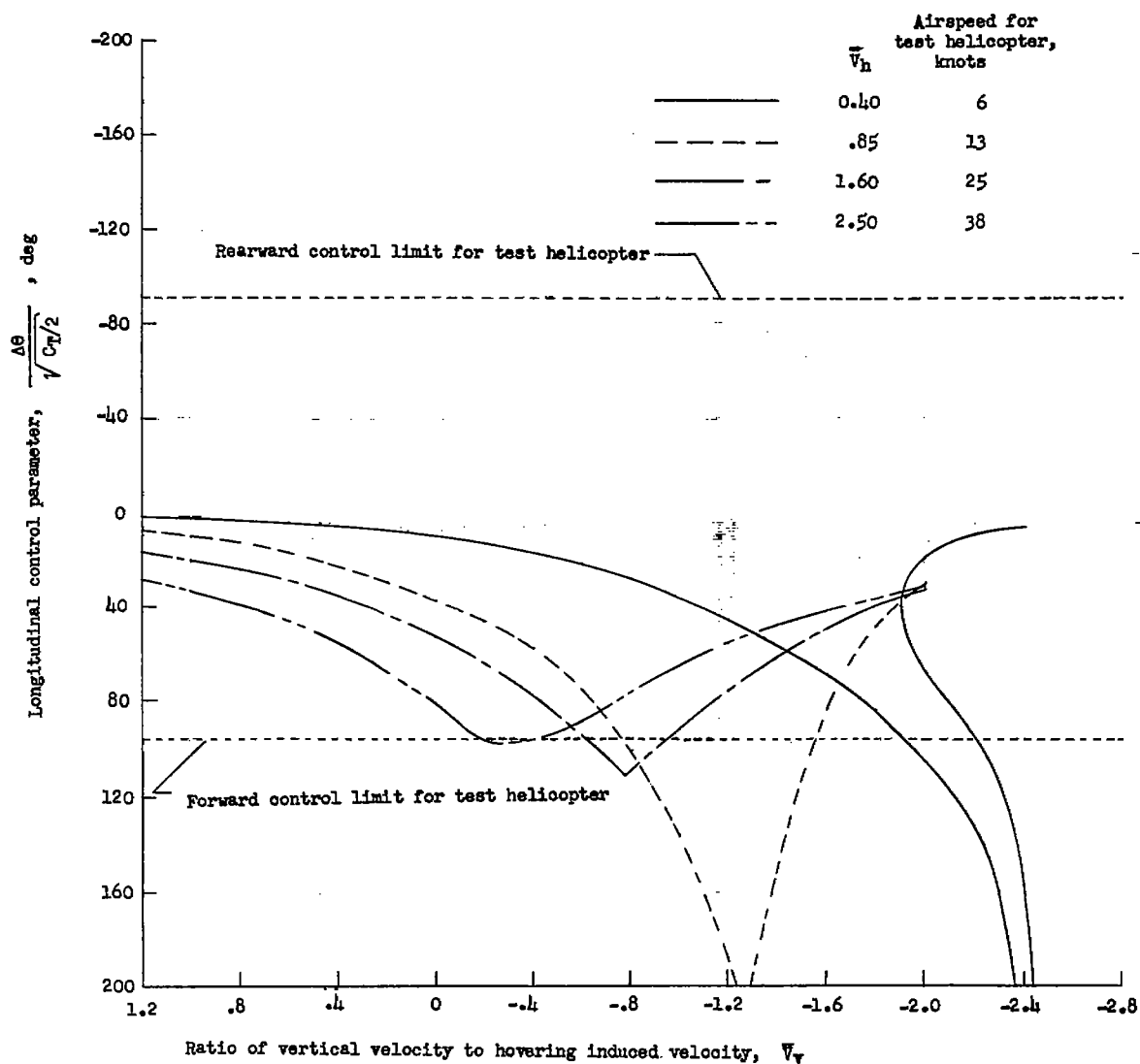
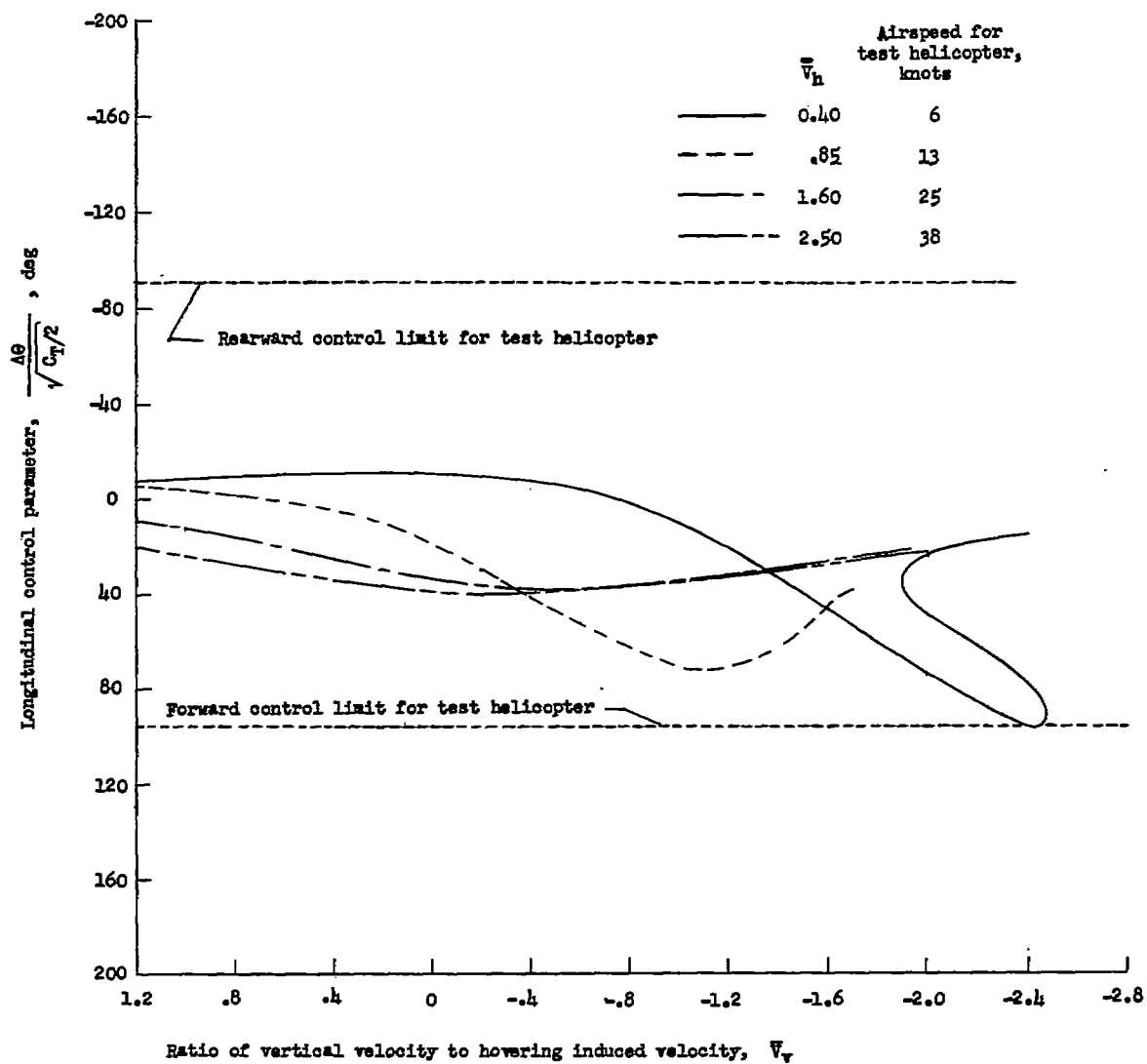(a) $\overline{V}_h$ = 0.85 fps (13 knots for test helicopter).
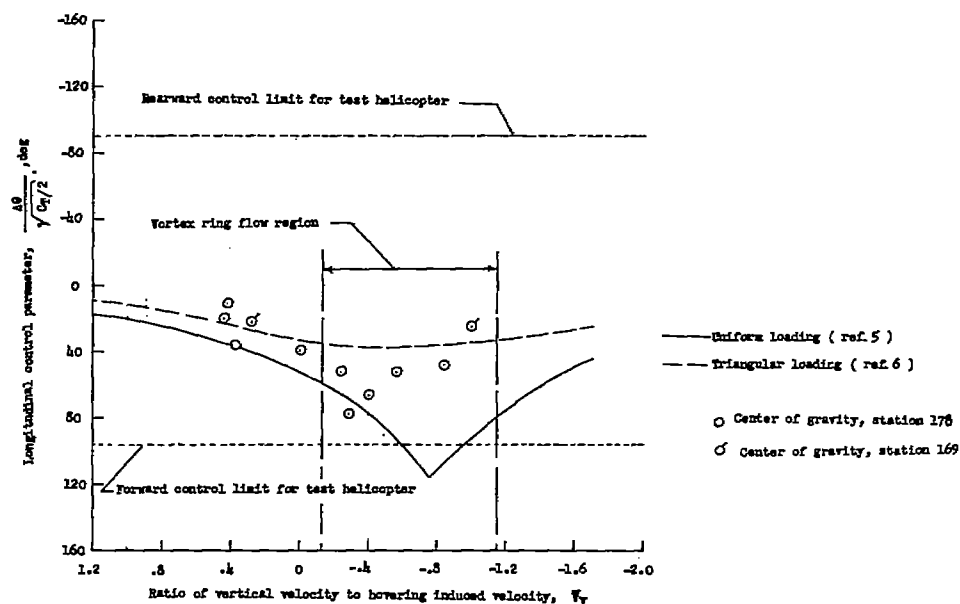
(b) $\overline{V}_h$ = 1.60 fps (25 knots for test helicopter).

Figure 7.- Comparison of measured and estimated variation of longi-
tudinal control positions.

(a) Interference based on uniform loading (ref. 5).

Figure 8.- Predicted variation of longitudinal control with vertical
velocity at several airspeeds.

(b) Interference based on triangular loading (ref. 6).
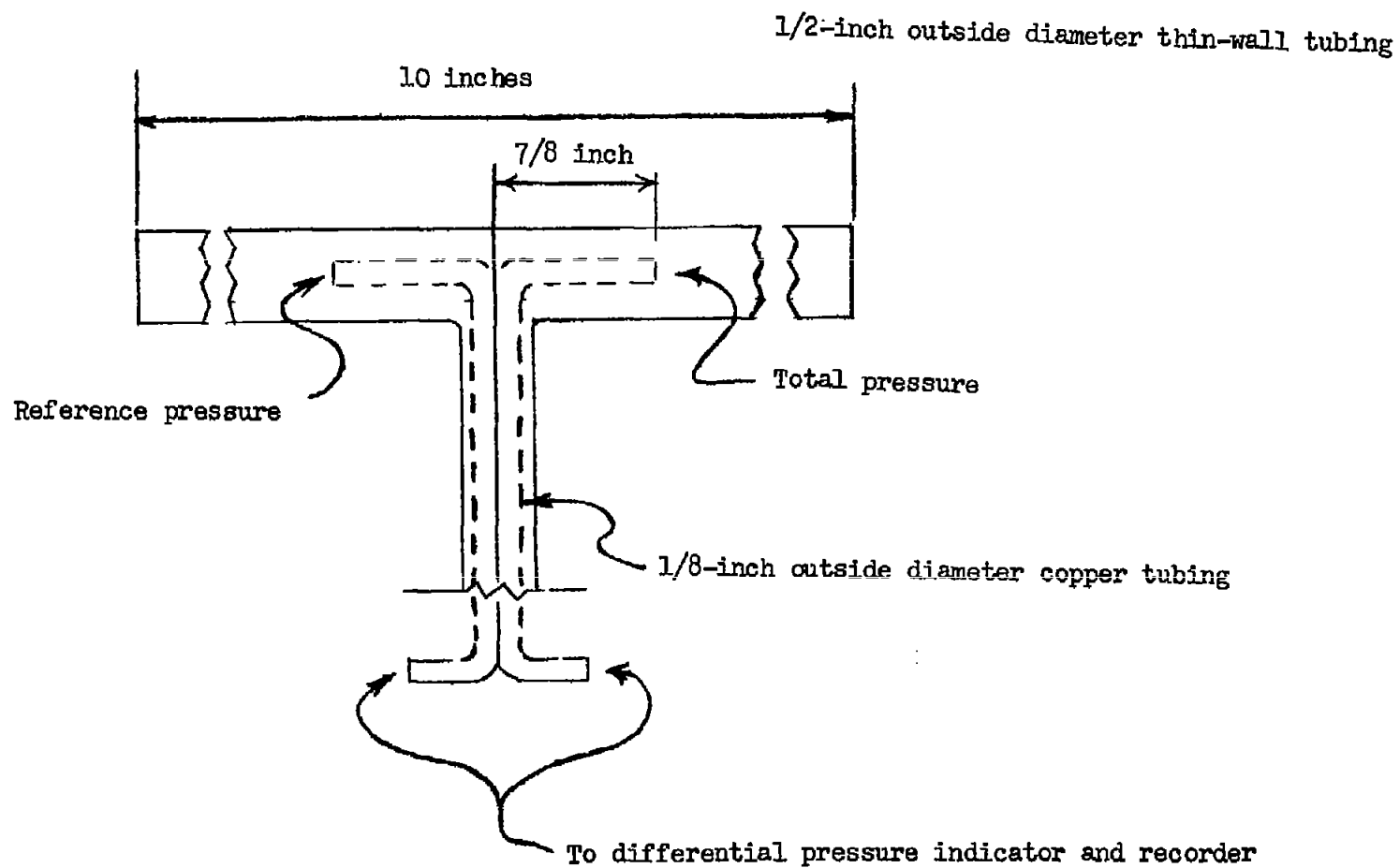
Figure 8.- Concluded.

1/2-inch outside diameter thin-wall tubing

10 inches

7/8 inch

Reference pressure

Total pressure

1/8-inch outside diameter copper tubing

To differential pressure indicator and recorder
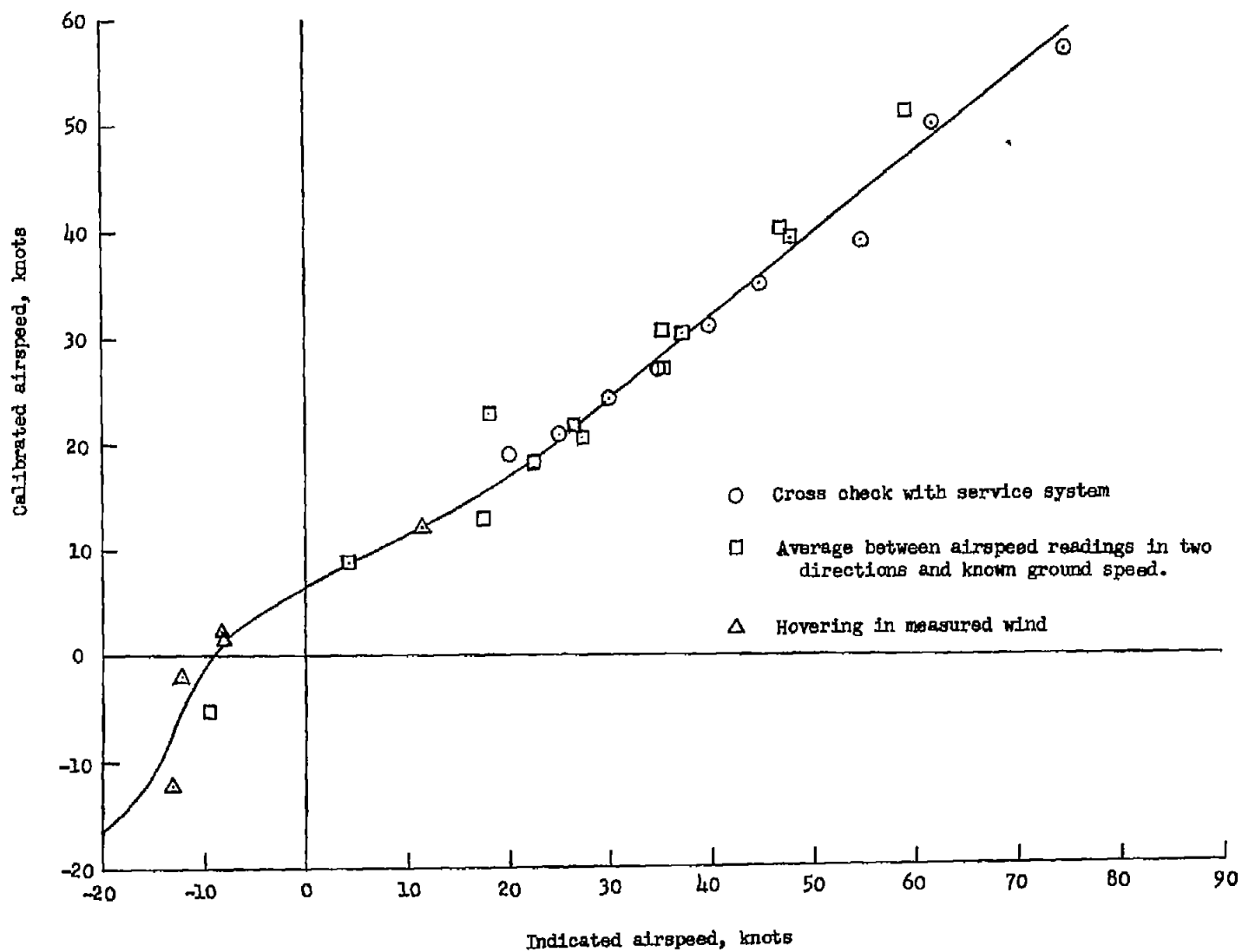
Figure 9.- Pressure pickup tubes for low-airspeed system.

Figure 10.- Calibration of low-airspeed system.